

# Science of the Total Environment

## Vibrio Harveyi exosomes secrete VgrG protein and cause toxic effects to *Ruditapes philippinarum*

--Manuscript Draft--

<b>Manuscript Number:</b>	STOTEN-D-24-40512
<b>Article Type:</b>	Research Paper
<b>Keywords:</b>	Vibrio Harveyi, toxic effect, proteomics
<b>Corresponding Author:</b>	Xiaoli Liu Ludong University CHINA
<b>First Author:</b>	Zimin Cai
<b>Order of Authors:</b>	Zimin Cai  Zihan Xing  Mingzhe Xu  Ruijia Tao  Liuya Mi  Jiawan Lv  Bowen Yang  Yancui Zhao  Lei Wang  Xiaoli Liu
<b>Abstract:</b>	Considering the potential role of valine-glycine repeat (VgrG) a core component of Type VI secretion system (T6SS) proteins secreted by exosomes in the pathogenicity of Vibrio harveyi, this study aimed to understand the mechanism of <i>V. harveyi</i> VgrG protein in bivalves. Ultra-centrifugation was used to extract <i>V. harveyi</i> exosomes which were fluorescently labelled to trace them; Then, Reactive oxygen species (ROS), cspase-3, superoxide dismutase (SOD), glutathione peroxidase (GPx) and malonaldehyde (MDA) were detected in hemocytes of <i>R. philippinarum</i> ; Protein changes were determined by 4D TOF Pro2 combined with DIA-PASEF mass spectrometry scanning mode after exposure to recombinant protein VgrG for 24 h. Our results showed that <i>V. harveyi</i> exosomes could enter host cells and exert toxic effects. VgrG interferes with the main metabolism and energy balance of <i>R. philippinarum</i> by inhibiting major energy metabolism pathways and protein synthesis, and inducing oxidative stress and apoptosis. The results proved that VgrG could be crucial to the functioning of T6SS proteins in <i>V. harveyi</i> and provided a new way to analyse Vibrio mechanisms from an exosome perspective.
<b>Suggested Reviewers:</b>	Hailong Zhou hlongzhou@163.com Professor Zhou works in Hainan University and is major in responses of marine invertebrates to their environment  Pengzhi Qi qpz2004@vip.sina.com Dr. Qi is major in immune mechanisms in bivalves  Weiwei Zhang zhangweiwei@nbu.edu.cn Prof Zhang is major in toxic effects of Vibrio  Chenglong Ji clji@yic.ac.cn Dr. Ji is major in marine environmental toxicity

	<p>Qiang Li chm_liq@ujn.edu.cn Prof. Li is major in environmental microorganism</p>
	<p>Huifeng Wu hfwu@yic.ac.cn Prof. Wu is major in aquatic toxicology</p>
<b>Opposed Reviewers:</b>	

2024-9-20

Damià Barceló, PhD

Co-Editors-in-Chief

*Science of the Total Environment*

Dear Editors:

I wish to submit an original article for publication in *Science of the Total Environment*, titled “*Vibrio Harveyi* exosomes secrete VgrG protein and cause toxic effects to *Ruditapes philippinarum*” The paper was coauthored by Zimin Cai, Zihan Xing, Mingzhe Xu, Ruijia Tao, Liuya Mi, Jiawan Lv, Bowen Yang, Yancui Zhao, Lei Wang, Xiaoli Liu.

Exosomes are effective carriers of intercellular information transmission, T6SS is deemed as "one of the most interesting areas" of microbiological research and VgrG is essential for T6SS. This study aimed to understand the mechanism of T6SS VgrG proteins secreted by *Vibrio harveyi* exosomes in bivalves. *V. harveyi* is a serious mariculture pathogen which triggers a series of inflammatory responses. We believe that our study makes a significant contribution to the literature because research on the effect *V. harveyi* VgrG proteins on bivalves is relatively lacking. Our study explored the pathogenic mechanism of *V. harveyi* from the perspective of exosome-secreted proteins and provided data for revealing the role of the VgrG protein.

Further, we believe that this paper will be of interest to the readership of your journal because the infections caused by *V. harveyi* lead to serious losses in the marine culture industry. Strengthening research on the pathogenic mechanisms of *V. harveyi* is essential for its prevention and treatment.

This manuscript has not been published or presented elsewhere in part or in entirety and is not under consideration by another journal. We have read and understood your journal's policies, and we believe that neither the manuscript nor the study violates any of these. There are no conflicts of interest to declare.

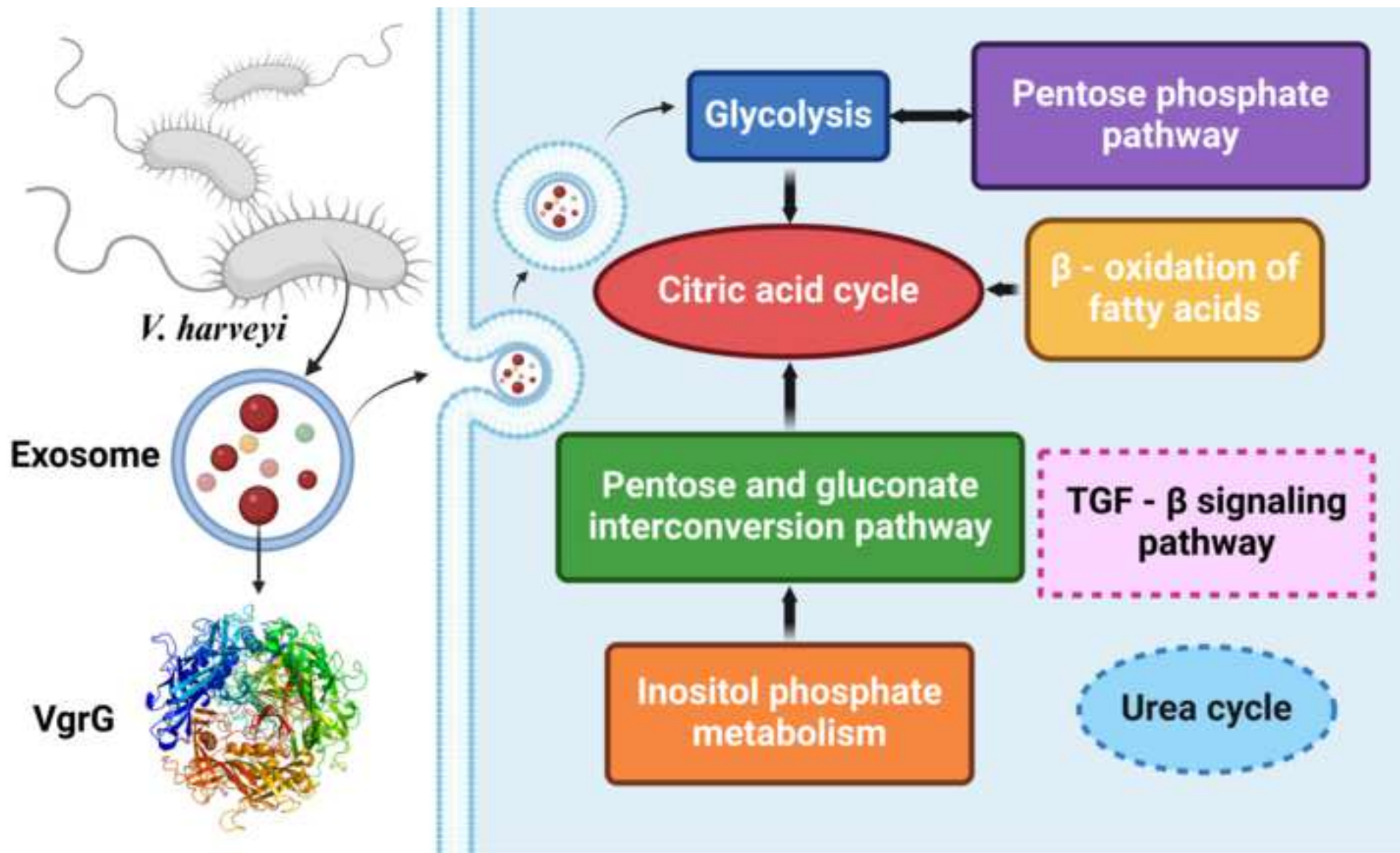
Thank you for your consideration and many thanks for your kind work. I look forward to hearing from you.

Sincerely,

Xiaoli Liu

Ludong University

lxlshz2006@163.com



## Highlights

- The mechanism of *Vibrio harveyi* VgrG proteins in bivalves was investigated
- *V. harveyi* exosomes could enter host cells and exert toxic effects
- VgrG interferes with the main metabolism and energy balance of *R. philippinarum*
- VgrG could be crucial to the functioning of T6SS proteins in *V. harveyi*
- We provide a new way to analyse Vibrio mechanisms from an exosome perspective

[Click here to view linked References](#)

1    ***Vibrio Harveyi* exosomes secrete VgrG protein and cause toxic effects to *Ruditapes*  
2    *philippinarum***

3    Zimin Cai<sup>a, #</sup>, Zihan Xing<sup>a, #</sup>, Mingzhe Xu<sup>a, #</sup>, Ruijia Tao<sup>a</sup>, Liuya Mi<sup>a</sup>, Jiawan Lv<sup>a</sup>, Bowen  
4    Yang<sup>b</sup>, Yancui Zhao<sup>a</sup>, Lei Wang<sup>a</sup>, Xiaoli Liu<sup>a,\*</sup>

5    <sup>a</sup> School of Life Sciences, Ludong University, Yantai 264025, P. R. China.

6    <sup>b</sup> Department of Chemistry, University of Alberta, Edmonton, Alberta T6G 2G2,  
7    Canada.

8

9    **Abstract**

10   Considering the potential role of valine-glycine repeat (VgrG) a core component of  
11   Type VI secretion system (T6SS) proteins secreted by exosomes in the pathogenicity  
12   of *Vibrio harveyi*, this study aimed to understand the mechanism of *V. harveyi* VgrG  
13   protein in bivalves. Ultra-centrifugation was used to extract *V. harveyi* exosomes which  
14   were fluorescently labelled to trace them; Then, Reactive oxygen species (ROS),  
15   cspase-3, superoxide dismutase (SOD), glutathione peroxidase (GPx) and  
16   malonaldehyde (MDA) were detected in hemocytes of *R. philippinarum*; Protein  
17   changes were determined by 4D TOF Pro2 combined with DIA-PASEF mass  
18   spectrometry scanning mode after exposure to recombinant protein VgrG for 24 h. Our  
19   results showed that *V. harveyi* exosomes could enter host cells and exert toxic effects.  
20   VgrG interferes with the main metabolism and energy balance of *R. philippinarum* by  
21   inhibiting major energy metabolism pathways and protein synthesis, and inducing  
22   oxidative stress and apoptosis. The results proved that VgrG could be crucial to the  
23   functioning of T6SS proteins in *V. harveyi* and provided a new way to analyse Vibrio  
24   mechanisms from an exosome perspective.

25   **Keywords**

26   *Vibrio Harveyi*, toxic effect, proteomics

27

28

29   <sup>#</sup>Zimin Cai, Zihan Xing, and Mingzhe Xu contributed equally to this work.

30   \* Corresponding author. E-mail address: lxlshz2006@163.com (Xiaoli Liu)

31     **1. Introduction**

32     *Vibrio harveyi*, an essential member of the Vibrionaceae family, is widely distributed  
33     in aquatic systems (Montánchez and Kaberdin, 2020). However it is a well-recognised  
34     and serious mariculture pathogen especially for invertebrates and fish which triggers a  
35     series of inflammatory responses (Zhang et al., 2020) (Morot et al., 2024) (Yu et al.,  
36     2022), eventually causing diseases such as acute hepatopancreatic necrosis, bacterial  
37     white tail, black shell, foot pustule, luminous vibriosis, skin ulceration and white patch  
38     diseases (Zhang et al., 2020) (Chen et al., 2024). These infection leads to serious losses  
39     in the marine culture industry (Nurhafizah et al., 2021) (Zhao et al., 2023).  
40     Strengthening research on the pathogenic mechanisms of *V. harveyi* is essential for its  
41     prevention and treatment.

42     Regarding pathogenic infections, bacterial exosomes play important roles in  
43     delivering virulence factors (Zhu et al., 2022). Exosomes—flat spheroids with a lipid  
44     bilayer structure and diameter of 30–150 nm—are effective carriers of intercellular  
45     information transmission (Johnstone et al., 1987) (Chahar et al., 2015) (Meckes, 2015).  
46     They are complex and contain various proteins, mRNAs, lipids, and other substances.  
47     The biological information carried by exosomes not only represents the state of the  
48     source tissue or cell but also participates in the regulation of a variety of biological  
49     processes of the recipient cell, such as microbial disease and immune and inflammatory  
50     responses (Boukouris and Mathivanan, 2015) (Zhang et al., 2015) (Hoshino et al., 2015)  
51     (Ying et al., 2017). Exosomal proteins of *V. Harveyi* contain toxic protein factors,  
52     including Type VI secretion system (T6SS) proteins (Chen et al., 2023).

53     T6SS proteins are used by bacteria to interfere with various physiological processes  
54     of host cells, and inject specific protein effectors to effectively invade the host or  
55     environment (He et al., 2023). T6SS—a recently discovered secretory system—is  
56     primarily found in gram-negative bacteria and is "one of the most interesting areas" of  
57     microbiological research (Aschtgen et al., 2010). T6SS is composed of three parts: the  
58     baseplate, tube sheath, and membrane complex. Owing to T6SS composition variations  
59     in different bacteria, the specific functions of many proteins remain unclear. Among  
60     these T6SS parts, valine-glycine repeat G (VgrG), which belongs to the baseplate

61 component, is essential for T6SS assembly (He et al., 2023) (Li et al., 2024) (Liang et  
62 al., 2023), and may attenuate the host defence response (Tighilt et al., 2022) (Pothula  
63 et al., 2023). VgrG1 from *Aeromonas hydrophila* induces host cell toxicity through  
64 ADP-ribosylation (Suarez et al., 2010). In *V. cholera*, VgrG may assemble a "cell-  
65 puncturing device" which destroys the host cells (Pukatzki et al., 2007). VgrG in  
66 *Chromobacterium violaceum* plays a key role in interbacterial competition (Alves et al.,  
67 2022). Recently, there has been research on VgrG protein effects on *V. harveyi*  
68 pathogenicity, which showed that the protein upregulates major histocompatibility  
69 complex class Ia, tumour necrosis factor- $\alpha$ , interferon  $\gamma$ , and cluster of differentiation  
70 4 in Epinephelus (Du et al., 2024). However, research on the effect *V. harveyi* VgrG  
71 proteins on bivalves is relatively lacking.

72 Considering the potential role of VgrG secreted by exosomes in *V. harveyi*  
73 pathogenicity, this study aimed to understand the mechanism of *V. harveyi* VgrG  
74 proteins in bivalves. First, we investigated whether *V. harveyi* exosomes could enter  
75 host cells, and second, as one of the exosome components of *V. harveyi*, what effects  
76 did VgrG proteins do on the haemocytes of bivalves. Based on the two questions, ultra  
77 centrifugation were used to extract exosomes of *V. harveyi*; exosomes were  
78 fluorescently labeled to trace them; Then, reactive oxygen species (ROS), cspase-3,  
79 superoxide dismutase (SOD), glutathione peroxidase (GPx) and malonaldehyde (MDA)  
80 were detected in hemocytes of *Ruditapes philippinarum*—an edible species of saltwater  
81 clam in the family Veneridae; and protein changes were determined by 4D tims TOF  
82 Pro2 combined with DIA-PASEF (data independent acquisition-parallel accumulation  
83 serial fragmentation) mass spectrometry scanning mode after exposed to VgrG protein  
84 of 24 hours. Thus, our study explored the pathogenic mechanism of *V. harveyi* from the  
85 perspective of exosome-secreted proteins and provided data for revealing the role of  
86 the VgrG protein.

## 87 **2. Materials and Methods**

### 88 **2.1 Culture and exosome extraction of *V. harveyi***

89 *V. harveyi* (MCCC1A00232) was purchased from the Marine Culture Collection in  
90 China. The monoclonal colonies of *V. harveyi* were placed into 5 mL liquid medium

91 (Marine broth 2216), formulated as 22.44 g marine broth 2216 solid powder added to  
92 600 mL ultrapure water. Then, the *V. harveyi* broth was shaken at 170 rpm for 12 h at  
93 28 °C until the OD<sub>600</sub> value reached 100. Subsequently the broth was inoculated into  
94 500 mL marine broth 2216 liquid medium and shaken persistently with a speed of 170  
95 rpm for 12 h at 28°C. Finally, the broth was centrifuged at 7000 × g for 10 min at 4 °C  
96 and the supernatant was collected for subsequent experiments. Exosomes from *V.*  
97 *harveyi* were extracted by ultra-centrifugation, and their shape was detected by  
98 transmission electron microscopy (Hitachi, HT-7800) (Chen et al., 2023).

99 **2.2 Exosome tracing**

100 Peripheral blood mononuclear cells (PBMCs) were cultured in DMEM (Hyclone,  
101 SH30243.1) containing 1 % double antibody and 10 % foetal bovine serum at 37 °C  
102 and 5 % CO<sub>2</sub> with saturated humidity. The cell culture medium was changed once every  
103 2 days. The exosome concentration was 25 µg/mL, and PKH67 (Umibio, UR52303)  
104 was used for dyeing. After the PBMCs were attached to the wall, the PKH67-stained  
105 exosomes were added to the cells, incubated together for 24 h, then washed thrice with  
106 PBS and fixed in 4 % paraformaldehyde for 30 min. The cells were dyed with DAPI  
107 for 10 min and imaged using a laser scanning confocal microscope (Leica Sp8).

108 **2.3 Recombinant expression of VgrG**

109 The plasmid was constructed from the pET-30 a (+) vector. The recombinant plasmid  
110 was transferred into *Escherichia coli* Rosetta (DE3) competent cells and coated onto  
111 liquid medium after heat shock. Then the monoclones were selected and cultured in  
112 liquid medium containing 30 µg/mL kanamycin and 34 µg/mL chloramphenicol. When  
113 the OD<sub>600</sub> reached 0.6, 0.5 mM IPTG was added to the liquid medium which was then  
114 cultured at 20 °C overnight and 37 °C for 6 h and finally centrifuged at 4000 rpm for  
115 10 min to collect bacteria and discard the supernatant. The bacteria were then dissolved  
116 in a buffer solution of 8 M Urea, 50 mM Tris-HCl, 300 mM NaCl, 0.1 % Triton X-100,  
117 and a pH of 8.0. The recombinant VgrG proteins were purified by a Ni<sup>2+</sup> chelating  
118 sepharose column, concentrated with PEG20000, and filtered with a 0.45 µm  
119 membrane. A liquid chromatography-mass spectrometer (Thermo, Q Exactive) was  
120 used to identify the VgrG proteins. Trypsin (Promega) was used for enzymolysis, and

121 a C18 reversed-phase chromatography column (Acclaim PepMap RSLC, 75  $\mu$ m  $\times$  25  
122 cm C18-2  $\mu$ m 100 A) was used for the liquid phase system.

123 **2.4 Experimental animals and exposure conditions**

124 *R. philippinarum* was obtained from a local Jiutian aquatic products market in Yantai,  
125 China. The length of the clams were 2.5-2.9 cm and were put in a plastic boxes with a  
126 length, width, and height of 60, 40 and 12 cm respectively. The clams were placed in  
127 tanks containing sea water with a volume of 9 L and fed with *Chlorella vulgaris Beij*  
128 (2 % tissue dry weight daily) for 7 days. The adaptive culture was continuously aerated,  
129 32 practical salinity units were used in the sea water, the temperature was 25 °C, and  
130 photoperiod conditions were set to natural.

131 After the adaptive culture, the clams were randomly divided into control and protein-  
132 exposed groups, with each group containing six individuals. The protein was injected  
133 into the muscle at a concentration of 0.5  $\mu$ g/ $\mu$ L, and after 24 h the haemolymph was  
134 collected for subsequent experiments.

135 **2.5 Determination of reactive oxygen species and apoptosis**

136 ROS were detected according to the assay kit instructions (Solarbio). The  
137 haemolymph of *R. philippinarum* were washed twice with PBS, resuspended with 1 mL  
138 DCFH-DA probe solution (10  $\mu$ M), and then incubated away from light for 20 min at  
139 37 °C and vortexed every 5 min. After being centrifuged at 1000  $\times$  g at 4 °C for 5 min  
140 and resuspended with 1 mL PBS, the samples were detected using a BD FACSCanto II  
141 flow cytometer. The results were analysed using FlowJo software.

142 Apoptosis was tested by the activity of caspase-3 using a Multiskan spectrum  
143 microplate spectrophotometer (Infinite M200, TECAN). Caspase-3 was detected  
144 according to the manufacturer's instructions (Nanjing Jiancheng Bioengineering  
145 Institute, G015-1), and the detection wavelength was 405 nm.

146 **2.6 Measurement of Enzyme activities and lipid peroxidation**

147 Antioxidant enzyme activity was measured using the Infinite M200  
148 spectrophotometer according to the manufacturer's protocols. Antioxidant enzymes  
149 included SOD (Nanjing Jiancheng Bioengineering Institute, A001-1) and GPx (Nanjing  
150 Jiancheng Bioengineering Institute, A005-1), whereas lipid peroxidation included

151 MDA (Nanjing Jiancheng Bioengineering Institute, A003-1). The detection  
152 wavelengths for SOD, GPx, and MDA were 450, 412, and 532 nm, respectively. The  
153 protein concentration was determined using the Coomassie Brilliant Blue method.

154 **2.7 Comparative proteomics**

155 The comparative proteomics after VgrG stress in hemolymph of *R. philippinarum*  
156 from control and VgrG stress was studied by using 4D tims TOF Pro2 combined with  
157 DIA-PASEF mass spectrometry scanning mode. The low-abundance protein was  
158 extracted from the hemocytes and enzymolized by trypsin. After desalting the  
159 enzymolysis peptide, the samples were identified by LC-MS/MS. DIA technology was  
160 used to collect mass spectrum data of each sample. Data were qualitatively and  
161 quantitatively analysed using Spectronaut Pulsar 16 analysis software.

162 **2.8 Statistical analysis**

163 All data were expressed as mean  $\pm$  standard deviation. Two-sided *t*-tests were  
164 performed between the control group and VgrG protein treatment group,  $p < 0.05$   
165 indicated statistical significance. The criterion for screening differential proteins was  $p$   
166  $< 0.05$ , fold changes (FC)  $\geq 1.2$  or FC  $\leq 1/1.2$ .

167 **3. Results**

168 **3.1 Characterization and tracing of exosomes**

169 Figure 1 shows transmission electron images of the exosomes in *V. harveyi*. The  
170 exosomes were typically saucer-shaped, indicating successful isolation from *V. harveyi*.  
171 Figure 2 shows the images of exosomes traced using a laser-scanning confocal  
172 microscope where it can be seen that the exosomes (stained with PKH67, green  
173 fluorescence) could enter the PBMC cells (stained with DAPI, blue fluorescence).

174 **3.2 Recombinant proteins properties**

175 Figure 3 shows clear reaction bands obtained by SDS-PAGE analysis of the  
176 recombinant VgrG proteins where protein separation was good. Figure 4 shows the  
177 two-stage mass spectrometry of the VgrG proteins. Mascot search results of the LC-  
178 MS analysis indicated a protein score of 3481, sequence coverage of 54 %, calculated  
179 pI value of 6.40, and nominal mass of 70364 kDa.

180 ExPASy software of the ProtScale program (<https://web.expasy.org/protscale/>) was

181 used to analyse the hydrophilicity/hydrophobicity of the VgrG proteins (Figure 5). The  
182 maximum hydrophobicity of the proteins was 1.978 (132), and the minimum  
183 hydrophilicity was -2.956 (490). In general, the hydrophilic amino acids were more  
184 than the hydrophobic amino acids, indicating that the VgrG proteins were hydrophilic.

185 VgrG protein tertiary structure prediction and analysis were done using SWISS-  
186 MODLE online software (<https://swissmodel.expasy.org/>) and PyMOL software  
187 (<https://pymol.org/2/>), and the results are shown in Figure 6. The tertiary structure of  
188 the VgrG protein is needle-like, with a height, length, and width of 162, 80, and 75 Å,  
189 respectively, which is mainly formed by random folding and winding.

### 190 **3.3 Reactive oxygen species, apoptosis, enzyme activities and lipid peroxidation**

191 Flow cytometry analysis showed that the VgrG protein significantly increased ROS  
192 levels. Figures 7A and 7B show that the VgrG protein significantly increased caspase-  
193 3 in the haemolymph of *R. philippinarum*.

194 Figure 8 shows the activities of SOD, GPx, and the content of MDA which were  
195 significantly decreased compared to the control group.

### 196 **3.4 Comparative proteomics**

197 In total, 1051 and 1048 proteins in the control and VgrG stress groups were identified  
198 in the haemolymph of *R. philippinarum*, respectively. Figure 9A shows the molecular  
199 weights of these proteins. The distribution of the number of peptide segments  
200 corresponding to each qualitative protein is shown in Figure 9B. Most proteins contain  
201 more than two peptide segments, conducive to increasing the accuracy and credibility  
202 of the quantitative results. The peptide lengths are shown in Figure 9C, and most of the  
203 peptides are in 7–20 amino acids.

204 There were 31 upregulated and 40 downregulated proteins after exposure to VgrG,  
205 the protein characters are shown in Table 1. The PCA results of the control and VgrG  
206 protein treatment groups are shown in Figure 10A, where there was good differentiation  
207 between the two groups. and the volcano plot of these significantly altered proteins is  
208 shown in Figure 10B. The differential proteins were sorted by p-value, and the top 50  
209 proteins clustered according to protein expression in Figure 10C.

210 Gene Ontology (GO) analysis was performed using the Gene Ontology Consortium

211 (<http://www.geneontology.org/>), which includes three ontologies: biological process  
212 (BP), cellular component (CC) and molecular function (MF).

213 The GO enrichment analysis of the top 20 proteins (10 ontologies with ListHits >1  
214 and lowest p-value were screened) are shown in Figure 11. In the upregulated proteins,  
215 BP included translation, maturation of LSU-rRNA from tricistronic rRNA,  
216 tricarboxylic acid cycle, and proteolysis; CC included ribosome, ribonucleoprotein  
217 complex, cytosolic large ribosomal subunit, and nucleus; MF included structural  
218 constituent of ribosome, GTP-binding, and metal ion binding. In the downregulated  
219 proteins, BP included DNA topological change; CC included cytoplasm and nucleus;  
220 MF included DNA topoisomerase type I, protein serine/threonine phosphatase activity,  
221 actin binding, ATP hydrolysis activity, ATP binding, transferase activity, RNA/DNA  
222 binding, zinc ion binding, and metal ion binding.

223 A KEGG enrichment analysis was done according to the KEGG database  
224 (<https://www.genome.jp/kegg/>), and the top 20 KEGG pathways are shown in Figure  
225 12. Upregulated proteins were involved in the following metabolic processes: citrate  
226 cycle; phenylalanine, tyrosine and tryptophan biosynthesis; tropane, piperidine and  
227 pyridine alkaloid biosynthesis; isoquinoline alkaloid biosynthesis; carbon fixation in  
228 photosynthetic organisms; arginine biosynthesis; phenylalanine metabolism; nicotinate  
229 and nicotinamide metabolism; propanoate metabolism; tyrosine metabolism; alanine,  
230 aspartate and glutamate metabolism; pyrimidine metabolism; regulation of actin  
231 cytoskeleton; ferroptosis; fat digestion and absorption; ribosome; MAPK signaling  
232 pathway – yeast. Downregulated proteins were involved in the following metabolic  
233 processes: caprolactam degradation, aminobenzoate degradation, glutathione  
234 metabolism, arginine biosynthesis, pentose phosphate pathway, butanoate metabolism,  
235 propanoate metabolism, fatty acid degradation, proteasome, RNA degradation,  
236 ubiquitin mediated proteolysis, TGF-beta signalling pathway, PI3K-Akt signaling  
237 pathway, autophagy, and long - term depression.

238 The differential proteins were analysed by selecting species/closely related species  
239 (blast e-value: 1e-5) in the STRING database (<https://string-db.org/>) to determine their  
240 interactions. There were many of these interactions, and the protein-protein interaction

241 network analysis is shown in Figure 13.

#### 242 **4. Discussion**

243 Since the first human case of *V. harveyi* infection was reported in 1989, there has  
244 been growing evidence that it can infect organism through wounds, and induced a series  
245 of inflammatory responses (Zhao et al., 2021) (Sun et al., 2022). The protein  
246 components of bacterial exosomes play key roles in their pathogenicity (Chen et al.,  
247 2023). During the inflammation process, whether bacterial exosomes are released and  
248 enter the host cell is a key link to exploring their therapeutic characteristics. Here, the  
249 release of exosomes from *V. harveyi* was clearly captured (shown in Figure 2), proving  
250 that they participated in host invasion.

251 As an important component of exosomes in *V. harveyi*, VgrG is located at the T6SS  
252 tip, and the VgrG protein structure predicted here is similar to the needle-like structure,  
253 which allows bacteria to function effectively when in contact with the host. The VgrG  
254 trimers are capped by proline-alanine-alanine-arginine repeat-motif proteins (Calder  
255 and Snyder, 2023). VgrG is not only a structural component of T6SS, but also an  
256 effector with multiple functions (Du et al., 2024). It is necessary for interbacterial  
257 competition in *C. violaceum* (Alves et al., 2022). The knockout of the *VgrG* gene affects  
258 chemotaxis, adhesion, and biofilm formation in *Pseudomonas plecoglossicida* (D.  
259 Yang et al., 2023).

260 *R. philippinarum* is an economically important shellfish bivalve in China that is  
261 mainly produced in Shandong Province (Chen et al., 2021). *V. harveyi* infection  
262 severely threatens the clam aquaculture industry and induces immune responses in  
263 haemocytes (Q. Yang et al., 2023). It is therefore important to fully understand the  
264 virulence mechanisms of *V. harveyi*. In our study, a series of changes were detected in  
265 the haemocytes of *R. philippinarum* after VgrG stress. VgrG disturbed energy  
266 metabolism including the tricarboxylic acid (TCA) cycle, glycolysis and pentose  
267 phosphate pathway (PPP). *V. harveyi* causes changes in the TCA cycle of *Crassostrea*  
268 *hongkongensis*, an essential metabolic pathway for energy generation (Scagliola et al.,  
269 2020) (Ma et al., 2022). Our study confirmed that VgrG upregulated the TCA cycle,  
270 indicating that the organism was in a state of serious energy deficiency. Meanwhile, the

upregulated TCA cycle produced large amounts of acetyl-CoA entering the glycolysis pathway, but the enzyme triosephosphate isomerase (H6UNP5) was inhibited; therefore, energy could not be effectively converted in *R. philippinarum*. PPP is a glucose-oxidising pathway and PPP-derived nicotinamide adenine dinucleotide phosphate (NADPH) supports the generation of ROS (TeSlaa et al., 2023). In our study, inhibition reduced NADPH production and lacked reductive power, making it difficult to cope with oxidative stress; thus, ROS levels increased.

ROS in animals is involved in direct antimicrobial activity against bacteria (Herb and Schramm, 2021). Here, ROS levels were significantly elevated in haemocytes of *R. philippinarum* after exposure to the VgrG protein. MDA, SOD, and GPx are good oxidative stress markers (Abedi et al., 2023) and *V. harveyi* elevates the MDA contents, SOD and GPx activities in *Plectropomus leopardus* (Yu et al., 2018). In our study, these three markers were all significantly decreased, indicating that VgrG induced oxidative stress in *R. philippinarum*. Furthermore, SOD plays a dual role in the ROS pathway (Wang et al., 2018), however, the two changes caused by VgrG require further investigation.

The interaction of pathogenic bacteria with caspase-3 can affect host cell and bacterial survival (Wall and McCormick, 2014), and there is a negative correlation between caspase-3 and serine/threonine-protein phosphatase in apoptosis (Zhu et al., 2018) (Beroske et al., 2021). In our study, whereas serine/threonine-protein phosphatase was downregulated in *R. philippinarum*, confirming this phenomenon. VgrG also effectively inhibited DNA replication, RNA transcription, protein folding and translation. The efficiency of protein synthesis was reduced, which further increased the energy burden on the organism.

## 5. Conclusion

In our limited study, we ascertained that the exosomes of *V. harveyi* could enter host cells and exert toxic effects, and that VgrG interfered with the metabolism and energy balance of *R. philippinarum* by inhibiting major energy metabolism and protein synthesis pathways, inducing oxidative stress and apoptosis (shown in Figure 14).

These results prove that VgrG is crucial for T6SS functioning in *V. harveyi* and

301 provide a new way to analyse Vibrio mechanisms from an exosome perspective, which  
302 is of great significance for Vibrio control in marine organisms. But the study of the toxic  
303 components of Vibrio exosomes is just the beginning, and it will be of great interest to  
304 study their interactions with the host in the future.

305 **Acknowledgements**

306 This work was supported by the National Natural Science Foundation of China (grant  
307 number 32070126), The Innovation Project for Graduate students of Ludong University  
308 (IPGS2024-066), Talent Induction Program for Youth Innovation Teams in Colleges  
309 and Universities of Shandong Province (2022-2024).

310 **References**

- 311 Abedi, A., Ghobadi, H., Sharghi, A., Iranpour, S., Fazlzadeh, M., Aslani, M.R., 2023.  
312 Effect of saffron supplementation on oxidative stress markers (MDA, TAC, TOS,  
313 GPx, SOD, and pro-oxidant/antioxidant balance): An updated systematic review  
314 and meta-analysis of randomized placebo-controlled trials. *Front. Med.*  
315 <https://doi.org/10.3389/fmed.2023.1071514>
- 316 Alves, J.A., Leal, F.C., Previato-Mello, M., da Silva Neto, J.F., 2022. A Quorum  
317 Sensing-Regulated Type VI Secretion System Containing Multiple Nonredundant  
318 VgrG Proteins Is Required for Interbacterial Competition in *Chromobacterium*  
319 *violaceum*. *Microbiol. Spectr.* <https://doi.org/10.1128/spectrum.01576-22>
- 320 Aschtgen, M.S., Gavioli, M., Dessen, A., Lloubès, R., Cascales, E., 2010. The SciZ  
321 protein anchors the enteroaggregative *Escherichia coli* Type VI secretion system  
322 to the cell wall. *Mol. Microbiol.* <https://doi.org/10.1111/j.1365-2958.2009.07028.x>
- 324 Beroske, L., Van den Wyngaert, T., Stroobants, S., Van der Veken, P., Elvas, F., 2021.  
325 Molecular imaging of apoptosis: The case of caspase-3 radiotracers. *Int. J. Mol.*  
326 *Sci.* <https://doi.org/10.3390/ijms22083948>
- 327 Boukouris, S., Mathivanan, S., 2015. Exosomes in bodily fluids are a highly stable  
328 resource of disease biomarkers. *Proteomics - Clin. Appl.*  
329 <https://doi.org/10.1002/prca.201400114>
- 330 Calder, A., Snyder, L.A.S., 2023. Diversity of the type VI secretion systems in the

- 331 Neisseria spp. *Microb. Genomics*. <https://doi.org/10.1099/mgen.0.000986>
- 332 Chahar, H.S., Bao, X., Casola, A., 2015. Exosomes and their role in the life cycle and  
333 pathogenesis of RNA viruses. *Viruses*. <https://doi.org/10.3390/v7062770>
- 334 Chen, L., Yu, F., Sun, S., Liu, X., Sun, Z., Cao, W., Liu, S., Li, Z., Xue, C., 2021.  
335 Evaluation indicators of *Ruditapes philippinarum* nutritional quality. *J. Food Sci.*  
336 *Technol.* <https://doi.org/10.1007/s13197-020-04796-6>
- 337 Chen, M., Wan, Q., Xu, M., Chen, Z., Guo, S., 2024. Transcriptome Analysis of Host  
338 Anti-Vibrio harveyi Infection Revealed the Pathogenicity of *V. harveyi* to  
339 American Eel (*Anguilla rostrata*). *Mar. Biotechnol.*  
340 <https://doi.org/10.1007/s10126-024-10298-9>
- 341 Chen, Q., Ma, B., Xu, M., Xu, H., Yan, Z., Wang, F., Wang, Y., Huang, Z., Yin, S.,  
342 Zhao, Y., Wang, L., Wu, H., Liu, X., 2023. Comparative proteomics study of  
343 exosomes in *Vibrio harveyi* and *Vibrio anguillarum*. *Microb. Pathog.*  
344 <https://doi.org/10.1016/j.micpath.2023.106174>
- 345 Du, X., Kang, M., Yang, C., Yao, X., Zheng, L., Wu, Y., Zhang, P., Zhang, H., Zhou,  
346 Y., Sun, Y., 2024. Construction and analysis of the immune effect of two different  
347 vaccine types based on *Vibrio harveyi* VgrG. *Fish Shellfish Immunol.*  
348 <https://doi.org/10.1016/j.fsi.2024.109494>
- 349 He, W., Wu, K., Ouyang, Z., Bai, Y., Luo, W., Wu, D., An, H., Guo, Y., Jiao, M., Qin,  
350 Q., Zhang, J., Wu, Y., She, J., Hwang, P.M., Zheng, F., Zhu, L., Wen, Y., 2023.  
351 Structure and assembly of type VI secretion system cargo delivery vehicle. *Cell*  
352 *Rep.* <https://doi.org/10.1016/j.celrep.2023.112781>
- 353 Herb, M., Schramm, M., 2021. Functions of ros in macrophages and antimicrobial  
354 immunity. *Antioxidants*. <https://doi.org/10.3390/antiox10020313>
- 355 Hoshino, A., Costa-Silva, B., Shen, T.L., Rodrigues, G., Hashimoto, A., Tesic Mark,  
356 M., Molina, H., Kohsaka, S., Di Giannatale, A., Ceder, S., Singh, S., Williams, C.,  
357 Soplop, N., Uryu, K., Pharmer, L., King, T., Bojmar, L., Davies, A.E., Ararso, Y.,  
358 Zhang, T., Zhang, H., Hernandez, J., Weiss, J.M., Dumont-Cole, V.D., Kramer,  
359 K., Wexler, L.H., Narendran, A., Schwartz, G.K., Healey, J.H., Sandstrom, P.,  
360 Jørgen Labori, K., Kure, E.H., Grandgenett, P.M., Hollingsworth, M.A., De Sousa,

- 361 M., Kaur, S., Jain, M., Mallya, K., Batra, S.K., Jarnagin, W.R., Brady, M.S.,  
362 Fodstad, O., Muller, V., Pantel, K., Minn, A.J., Bissell, M.J., Garcia, B.A., Kang,  
363 Y., Rajasekhar, V.K., Ghajar, C.M., Matei, I., Peinado, H., Bromberg, J., Lyden,  
364 D., 2015. Tumour exosome integrins determine organotropic metastasis. Nature.  
365 <https://doi.org/10.1038/nature15756>
- 366 Johnstone, R.M., Adam, M., Hammond, J.R., Orr, L., Turbide, C., 1987. Vesicle  
367 formation during reticulocyte maturation. Association of plasma membrane  
368 activities with released vesicles (exosomes). J. Biol. Chem.  
369 [https://doi.org/10.1016/s0021-9258\(18\)48095-7](https://doi.org/10.1016/s0021-9258(18)48095-7)
- 370 Li, W., Huang, X., Li, D., Liu, X., Jiang, X., Bian, X., Li, X., Zhang, J., 2024. A  
371 combination of genomics and transcriptomics provides insights into the  
372 distribution and differential mRNA expression of type VI secretion system in  
373 clinical *Klebsiella pneumoniae*. mSphere.  
374 <https://doi.org/10.1128/msphere.00822-23>
- 375 Liang, X., Zheng, H.Y., Zhao, Y.J., Zhang, Y.Q., Pei, T.T., Cui, Y., Tang, M.X., Xu,  
376 P., Dong, T., 2023. VgrG Spike Dictates PAAR Requirement for the Assembly of  
377 the Type VI Secretion System. J. Bacteriol. <https://doi.org/10.1128/jb.00356-22>
- 378 Ma, L., Lu, J., Yao, T., Ye, L., Wang, J., 2022. Gender-Specific Metabolic Responses  
379 of *Crassostrea hongkongensis* to Infection with *Vibrio harveyi* and  
380 Lipopolysaccharide. Antioxidants. <https://doi.org/10.3390/antiox11061178>
- 381 Meckes, D.G., 2015. Exosomal Communication Goes Viral. J. Virol.  
382 <https://doi.org/10.1128/jvi.02470-14>
- 383 Montánchez, I., Kaberdin, V.R., 2020. *Vibrio harveyi*: A brief survey of general  
384 characteristics and recent epidemiological traits associated with climate change.  
385 Mar. Environ. Res. <https://doi.org/10.1016/j.marenvres.2019.104850>
- 386 Morot, A., Delavat, F., Bazire, A., Paillard, C., Dufour, A., Rodrigues, S., 2024. Genetic  
387 Insights into Biofilm Formation by a Pathogenic Strain of *Vibrio harveyi*.  
388 Microorganisms. <https://doi.org/10.3390/microorganisms12010186>
- 389 Nurhafizah, W.W.I., Lee, K.L., Laith A., A.R., Nadirah, M., Danish-Daniel, M.,  
390 Zainathan, S.C., Najiah, M., 2021. Virulence properties and pathogenicity of

- 391 multidrug-resistant *Vibrio harveyi* associated with luminescent vibriosis in Pacific  
392 white shrimp, *Penaeus vannamei*. J. Invertebr. Pathol.  
393 <https://doi.org/10.1016/j.jip.2021.107594>
- 394 Pothula, R., Lee, M.W., Patricia Stock, S., 2023. Type 6 secretion system components  
395 hcp and vgrG support mutualistic partnership between *Xenorhabdus bovienii*  
396 symbiont and *Steinernema jolleti* host. J. Invertebr. Pathol.  
397 <https://doi.org/10.1016/j.jip.2023.107925>
- 398 Pukatzki, S., Ma, A.T., Revel, A.T., Sturtevant, D., Mekalanos, J.J., 2007. Type VI  
399 secretion system translocates a phage tail spike-like protein into target cells where  
400 it cross-links actin. Proc. Natl. Acad. Sci. U. S. A.  
401 <https://doi.org/10.1073/pnas.0706532104>
- 402 Scagliola, A., Mainini, F., Cardaci, S., 2020. The tricarboxylic acid cycle at the  
403 crossroad between cancer and immunity. Antioxidants Redox Signal.  
404 <https://doi.org/10.1089/ars.2019.7974>
- 405 Suarez, G., Sierra, J.C., Erova, T.E., Sha, J., Horneman, A.J., Chopra, A.K., 2010. A  
406 type VI secretion system effector protein, VgrG1, from *Aeromonas hydrophila*  
407 that induces host cell toxicity by ADP ribosylation of actin. J. Bacteriol.  
408 <https://doi.org/10.1128/JB.01260-09>
- 409 Sun, Z., Liu, X., Lu, M., Zhang, X., Sun, J., 2022. Serum-derived exosomes induce  
410 proinflammatory cytokines production in *Cynoglossus semilaevis* via miR-133-3p.  
411 Dev. Comp. Immunol. <https://doi.org/10.1016/j.dci.2022.104497>
- 412 TeSlaa, T., Ralser, M., Fan, J., Rabinowitz, J.D., 2023. The pentose phosphate pathway  
413 in health and disease. Nat. Metab. <https://doi.org/10.1038/s42255-023-00863-2>
- 414 Tighilt, L., Boulila, F., De Sousa, B.F.S., Giraud, E., Ruiz-Argüeso, T., Palacios, J.M.,  
415 Imperial, J., Rey, L., 2022. The *Bradyrhizobium* Sp. LmicA16 Type VI Secretion  
416 System Is Required for Efficient Nodulation of *Lupinus* Spp. Microb. Ecol.  
417 <https://doi.org/10.1007/s00248-021-01892-8>
- 418 Wall, D.M., McCormick, B.A., 2014. Bacterial secreted effectors and caspase-3  
419 interactions. Cell. Microbiol. <https://doi.org/10.1111/cmi.12368>
- 420 Wang, Y., Branicky, R., Noë, A., Hekimi, S., 2018. Superoxide dismutases: Dual roles

- 421       in controlling ROS damage and regulating ROS signaling. J. Cell Biol.  
422       <https://doi.org/10.1083/jcb.201708007>
- 423       Yang, D., Zhao, L., Li, Q., Huang, L., Qin, Y., Wang, P., Zhu, C., Yan, Q., 2023. The  
424       involvement of the T6SS vgrG gene in the pathogenicity of *Pseudomonas*  
425       *plecoglossicida*. J. Fish Dis. <https://doi.org/10.1111/jfd.13829>
- 426       Yang, Q., Xiao, G., Chen, R., Huang, X., Teng, S., 2023. Immune responses of  
427       hemocytes in the blood clam *Tegillarca granosa* in response to in vivo *Vibrio*  
428       *harveyi* infection.              Fish              Shellfish              Immunol.  
429       <https://doi.org/10.1016/j.fsi.2022.11.035>
- 430       Ying, W., Riopel, M., Bandyopadhyay, G., Dong, Y., Birmingham, A., Seo, J.B.,  
431       Ofrecio, J.M., Wollam, J., Hernandez-Carretero, A., Fu, W., Li, P., Olefsky, J.M.,  
432       2017. Adipose Tissue Macrophage-Derived Exosomal miRNAs Can Modulate in  
433       Vivo       and       in       Vitro       Insulin       Sensitivity.       Cell.  
434       <https://doi.org/10.1016/j.cell.2017.08.035>
- 435       Yu, G., Yu, H., Yang, Q., Wang, J., Fan, H., Liu, G., Wang, L., Bello, B.K., Zhao, P.,  
436       Zhang, H., Dong, J., 2022. *Vibrio harveyi* infections induce production of  
437       proinflammatory cytokines in murine peritoneal macrophages via activation of  
438       p38 MAPK and NF-κB pathways, but reversed by PI3K/AKT pathways. Dev.  
439       Comp. Immunol. <https://doi.org/10.1016/j.dci.2021.104292>
- 440       Yu, W., Wen, G., Lin, H., Yang, Y., Huang, X., Zhou, C., Zhang, Z., Duan, Y., Huang,  
441       Z., Li, T., 2018. Effects of dietary *Spirulina platensis* on growth performance,  
442       hematological and serum biochemical parameters, hepatic antioxidant status,  
443       immune responses and disease resistance of Coral trout *Plectropomus leopardus*  
444       (Lacepede, 1802).              Fish              Shellfish              Immunol.  
445       <https://doi.org/10.1016/j.fsi.2018.01.024>
- 446       Zhang, L., Zhang, S., Yao, J., Lowery, F.J., Zhang, Q., Huang, W.C., Li, P., Li, M.,  
447       Wang, X., Zhang, C., Wang, H., Ellis, K., Cheerathodi, M., McCarty, J.H.,  
448       Palmieri, D., Saunus, J., Lakhani, S., Huang, S., Sahin, A.A., Aldape, K.D., Steeg,  
449       P.S., Yu, D., 2015. Microenvironment-induced PTEN loss by exosomal  
450       microRNA primes brain metastasis outgrowth.       Nature.

451 https://doi.org/10.1038/nature15376

452 Zhang, X.H., He, X., Austin, B., 2020. *Vibrio harveyi*: a serious pathogen of fish and  
453 invertebrates in mariculture. Mar. Life Sci. Technol.  
454 https://doi.org/10.1007/s42995-020-00037-z

455 Zhao, N., Jia, L., He, X., Zhang, B., 2021. Proteomics of mucosal exosomes of  
456 *Cynoglossus semilaevis* altered when infected by *Vibrio harveyi*. Dev. Comp.  
457 Immunol. https://doi.org/10.1016/j.dci.2021.104045

458 Zhao, N., Jia, L., Wang, Q., Deng, Q., Ru, X., Zhu, C., Zhang, B., 2023. The feasibility  
459 of skin mucus replacing exosome as a pool for bacteria-infected markers  
460 development via comparative proteomic screening in teleost. Fish Shellfish  
461 Immunol. https://doi.org/10.1016/j.fsi.2022.108483

462 Zhu, J., Ji, Y., Yu, Y., Jin, Y., Zhang, X., Zhou, J., Chen, Y., 2018. Knockdown of  
463 serine/threonine protein phosphatase 5 enhances gemcitabine sensitivity by  
464 promoting apoptosis in pancreatic cancer cells in vitro. Oncol. Lett.  
465 https://doi.org/10.3892/ol.2018.8363

466 Zhu, T., Kong, M., Li, C., Shao, C., 2022. Exosomal miRNAs in the plasma of  
467 *Cynoglossus semilaevis* infected with *Vibrio harveyi*: Pleiotropic regulators and  
468 potential biomarkers involved in inflammatory and immune responses. Front.  
469 Immunol. https://doi.org/10.3389/fimmu.2022.949670

470

Table 1 List of the proteins differently expressed in haemocytes of *R. philippinarum* under VgrG treatment for 24 h

Accession number	Protein name	MW/kDa	Protein score	Sequence coverage (%)	Peptide numbers	Changes
A0A9D4JQG	Uncharacterized protein	21.75	55.80	20.89	5	↑
A0A9D4D0Z7	5'-nucleotidase	65.12	30.55	11.69	1	↑
A0A9D4J7V1	Friend leukemia integration 1 transcription factor	85.77	32.05	16.02	1	↑
A0A9D3Z553	60S ribosomal protein L7	28.51	54.58	19.47	6	↑
C8CBN2	Peptidyl-prolyl cis-trans isomerase	20.15	53.98	20.00	8	↑
A0A9D4KV93	Neuroendocrine convertase 2	72.95	50.82	15.35	1	↑
A0A9D4JRV0	Succinate dehydrogenase [ubiquinone] iron-sulfur subunit, mitochondrial	32.30	55.99	18.24	1	↑
A0A9D4GLT5	Succinate--CoA ligase [GDP-forming] subunit beta, mitochondrial	46.31	51.37	17.73	1	↑
A0A9D4M7Z3	LSM domain-containing protein	62.46	31.73	13.20	1	↑
A0A9D4E5F0	Aspartate aminotransferase	48.38	52.43	17.23	2	↑
A0A9D4E4J1	Alpha-1,4 glucan phosphorylase	9.25	38.75	16.05	1	↑
A0A9D3YP01	40S ribosomal protein S19	34.71	50.31	19.72	2	↑
A0A9D3Z382	Large ribosomal subunit protein uL5 C-terminal domain-containing protein	14.46	53.82	17.80	2	↑
A0A9D3Z553	60S ribosomal protein L7	28.51	54.58	19.47	6	↑
A0A9D4BR86	60S ribosomal protein L35	10.02	52.07	18.10	1	↑
A0A9D4CH97	Large ribosomal subunit protein uL13	23.17	47.47	17.46	1	↑
A0A9D4IAB1	40S ribosomal protein S26	14.14	52.45	19.63	2	↑
A0A9D4LP06	Ribosomal protein L3	46.17	57.06	19.45	2	↑
A0A9D4L8G5	Protein transport protein SEC23	86.42	53.14	16.50	3	↑

A0A9D4DBY2	Coiled-coil domain-containing protein 25	24.49	55.45	17.28	3	↑
A0A9D4CAE0	Secernin-2	38.52	54.89	17.91	1	↑
A0A067XI00	Ferritin	26.52	58.86	22.81	8	↑
A0A3G4ZKV7	Histone 1.B	18.75	52.95	20.62	1	↑
A0A9D4JQG1	Uncharacterized protein	21.75	55.80	18.25	1	↑
A0A9D4E5F0	Aspartate aminotransferase	48.38	52.43	17.23	2	↑
A0A9D4D0Z7	5'-nucleotidase	65.12	30.55	11.69	1	↑
A0A1P8SD50	Macin	9.48	48.64	19.17	1	↑
A0A9D4IG13	DNA topoisomerase I	112.39	44.66	10.55	1	↓
A0A9D4N8M0	DNA topoisomerase	96.80	38.10	13.87	1	↓
A0A9D4CLQ7	Serine/threonine-protein phosphatase	35.09	56.18	15.84	2	↓
A0A9D4LR63	Serine/threonine-protein phosphatase	35.44	56.50	18.72	2	↓
A0A9D4LE94	Calponin-homology (CH) domain-containing protein	10.79	47.58	16.75	2	↓
A0A9D4N3U3	Huntingtin interacting protein 1	122.71	54.86	16.18	1	↓
D8L792	Myosin heavy chain type II	23.81	51.83	18.18	1	↓
A0A1P8LJ43	Mothers against decapentaplegic homolog	51.17	53.29	14.30	2	↓
A0A9D3YRZ6	T-complex protein 1 subunit epsilon	59.95	56.93	19.22	6	↓
A0A9D4HEI1	Proteasome subunit beta	22.95	57.01	17.60	2	↓
A0A9D4HZ43	RRM domain-containing protein	70.21	57.48	19.21	6	↓
A0A9D4L693	B box-type domain-containing protein	62.07	42.47	10.55	1	↓
A0A9D4NCU3	Argininosuccinate lyase	52.84	37.95	10.55	1	↓
A0A9D4BJE8	ATPase AAA-type core domain-containing protein	7.80	55.56	19.17	5	↓
A0A9D4HDK1	AAA+ ATPase domain-containing protein (Fragment)	61.02	56.24	21.46	1	↓
A0A9D4C0Z6	Carboxypeptidase	54.35	49.76	18.45	1	↓
A0A9D4NGH1	Glucose-6-phosphate 1-dehydrogenase	60.16	55.47	18.52	4	↓
A0A9D4DRH6	UBC core domain-containing protein	20.57	51.17	15.89	1	↓

A0A9D4J6E5	RNA helicase	50.40	49.94	18.47	3	↓
H6UNP5	Triosephosphate isomerase (Fragment)	22.93	51.17	20.11	1	↓
A0A9D4RMX5	Tubulin polymerization-promoting protein family member 3	20.08	49.52	16.21	1	↓
H6B8N8	Sigma class glutathione S-transferase	23.22	50.81	11.86	2	↓
A0A2Z5ZC64	Retinoid X receptor	50.17	44.40	12.28	2	↓
A0A9D4HM55	Coatomer subunit beta	111.94	49.89	15.75	2	↓
A0A9D4BL79	Ribonuclease II/R domain-containing protein	299.59	50.79	15.22	1	↓
A0A9D4DR43	PABC domain-containing protein	14.45	55.52	14.21	1	↓
A0A1L1ZLS5	Alpha-amylase	57.68	43.66	10.55	2	↓
A0A2R4RNA7	Se-GPx-a	22.25	52.45	15.72	4	↓
A0A9D4CG08	Alpha-2-macroglobulin bait region domain-containing protein	79.38	55.06	19.15	2	↓
A0A9D4BXN7	MPN domain-containing protein	31.17	53.56	19.03	3	↓
A0A9D4B6D9	Enoyl-CoA hydratase	28.38	52.98	16.74	1	↓
A0A9D4DXX7	Fibronectin type-III domain-containing protein	78.00	49.82	17.29	2	↓
A0A9D3YN34	Uncharacterized protein	48.12	44.06	10.55	1	↓

## Figure captions

**Figure 1** Transmission electron micrographs image of exosomes in *V. harveyi*

**Figure 2** Images of exosome tracing by laser scanning confocal microscope. PBMC cells were stained with DAPI (blue fluorescence), exosomes were stained with PKH67 (green fluorescence)

**Figure 3** SDS-PAGE analysis of the recombinant protein VgrG. M: protein molecular standard; 1. Uninduced bacterial lysates; 2. Supernate at 20 °C; 3. Precipitation at 20 °C; 4. Supernate at 37 °C; 5. Precipitation at 37 °C; 6. Sample loading; 7. Outflow; 8. 20 mM imidazole; 9. 50 mM imidazole; 10. 500 mM imidazole; 11. Purified protein of VgrG

**Figure 4** Two-stage mass spectrometry of the VgrG protein

**Figure 5** The hydrophilicity/hydrophobicity of the VgrG protein

**Figure 6** Tertiary structure of the VgrG protein

**Figure 7** ROS and caspase-3 levels on haemocytes in the control and VgrG-treated groups of *R. philippinarum*. A. Flow cytometry analysis show the ROS results; B. caspase-3 detection. \* indicates statistical significance,  $p < 0.05$

**Figure 8** SOD and GPx activities and MDA content in the control and VgrG-treated groups of *R. philippinarum*. \* indicates statistical significance,  $p < 0.05$

**Figure 9** Molecular weight, peptide number, and peptide length of proteins

**Figure 10** A. PCA analysis between the control and VgrG-treatment groups; B. Volcano plot of the control and VgrG-treatment groups: red and blue represent high- and low-expression proteins, respectively, and each line represents the expression amount of each protein in the control and VgrG-treatment groups; C. Clustering heat map of proteins

**Figure 11** GO enrichment analysis of the top 30 proteins (10 ontologies with ListHits  $> 1$  and lowest p-value were screened)

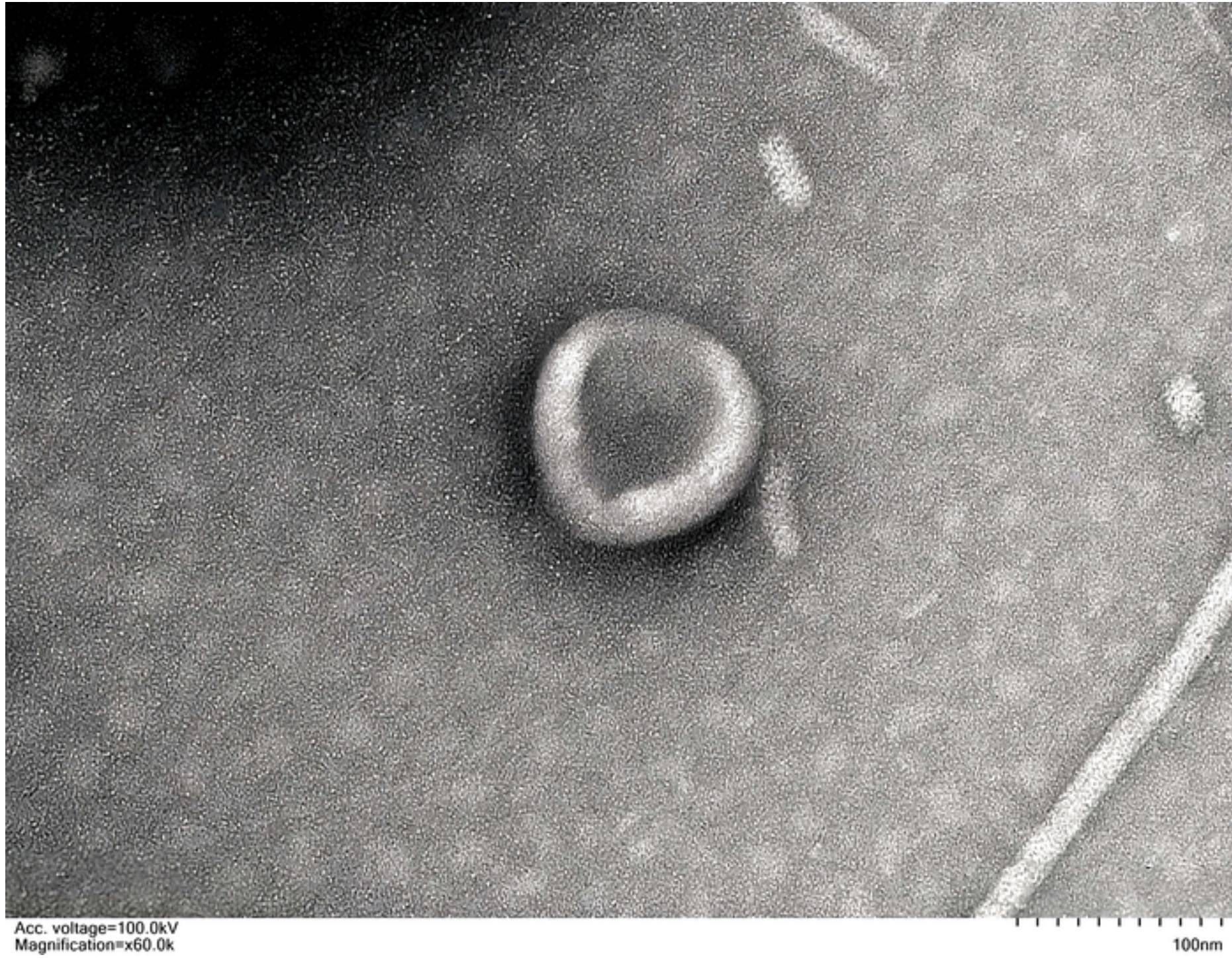
**Figure 12** KEGG enrichment analysis of the top 20 pathways (with the minimum p value)

**Figure 13** Protein-protein interactions

**Figure 14** The integrated changes of *R. philippinarum* after exposed to VgrG protein

Figure 1

[Click here to access/download;Figure;Figure 1.tif](#) 



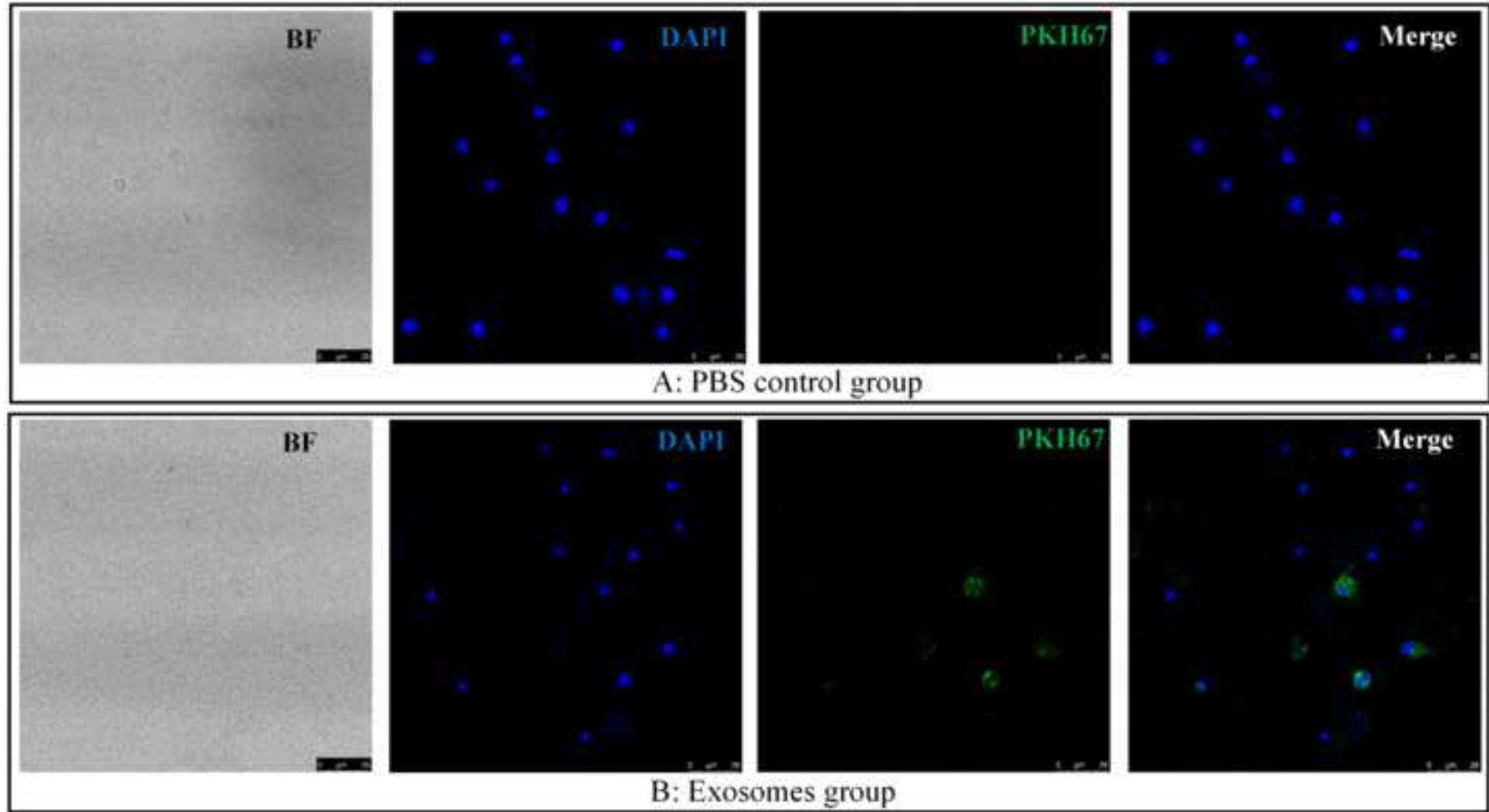


Figure 3

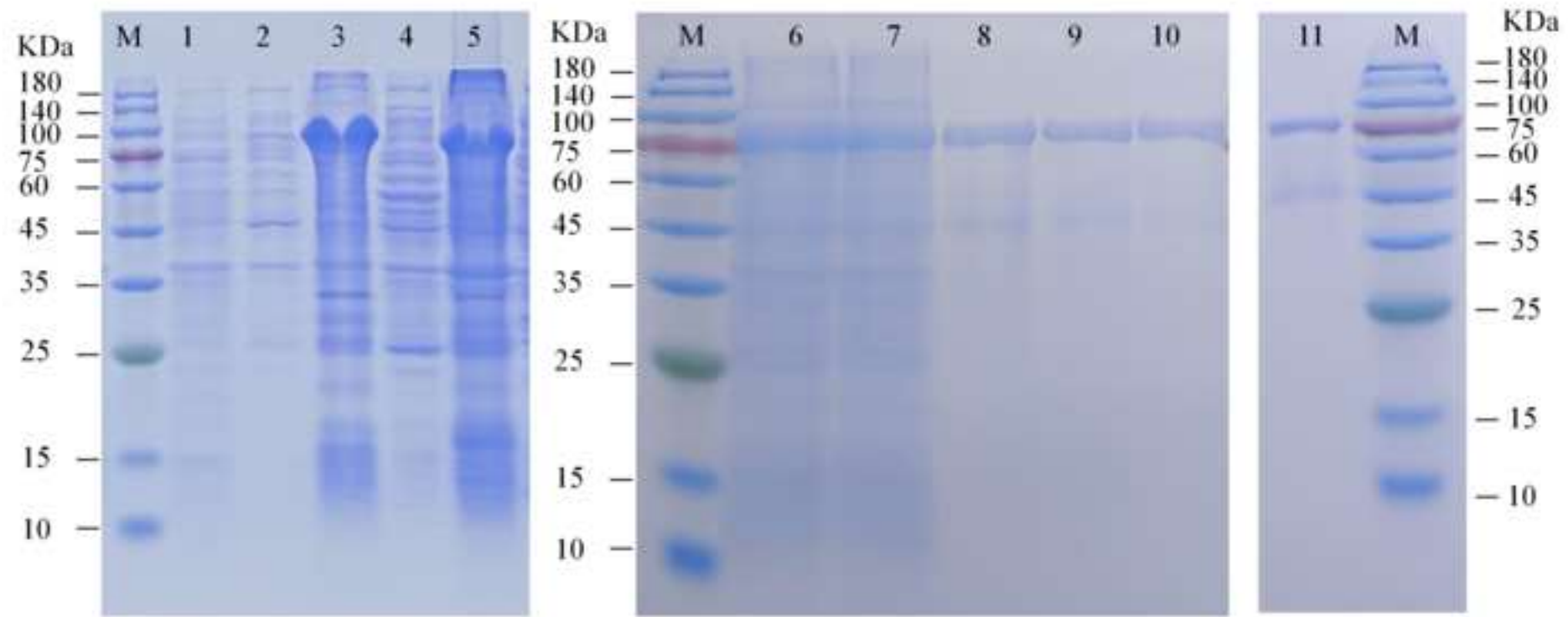
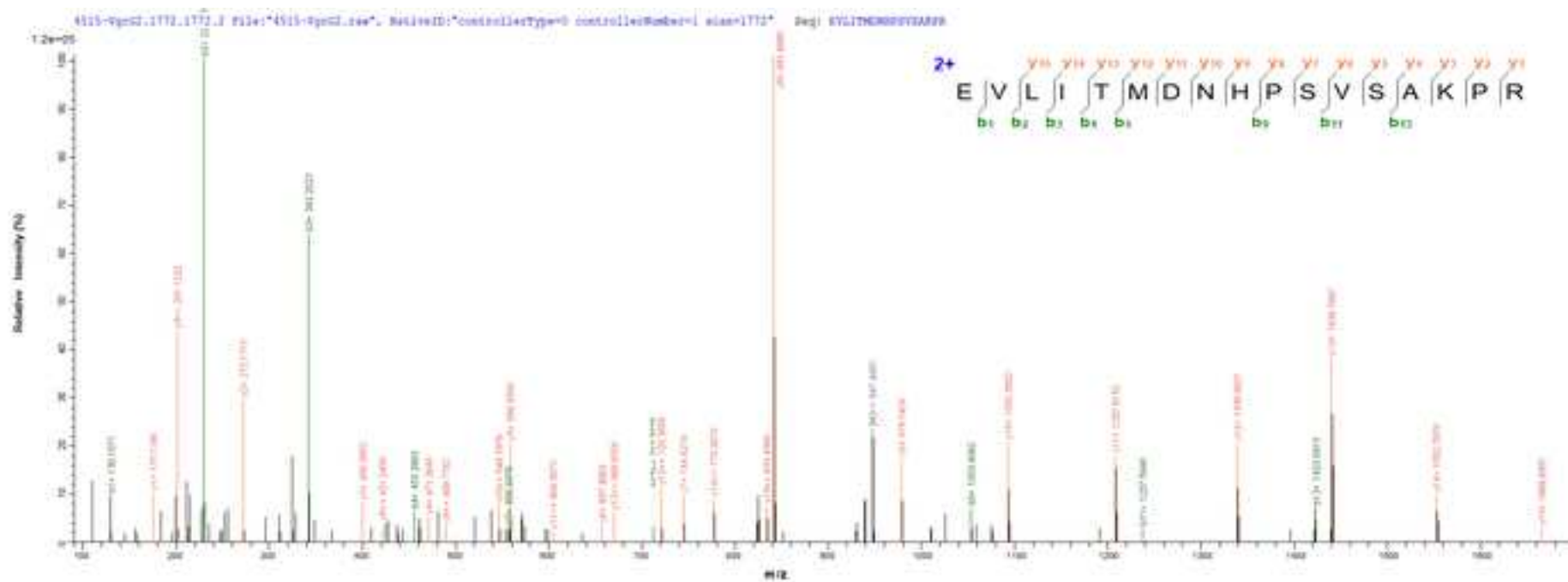
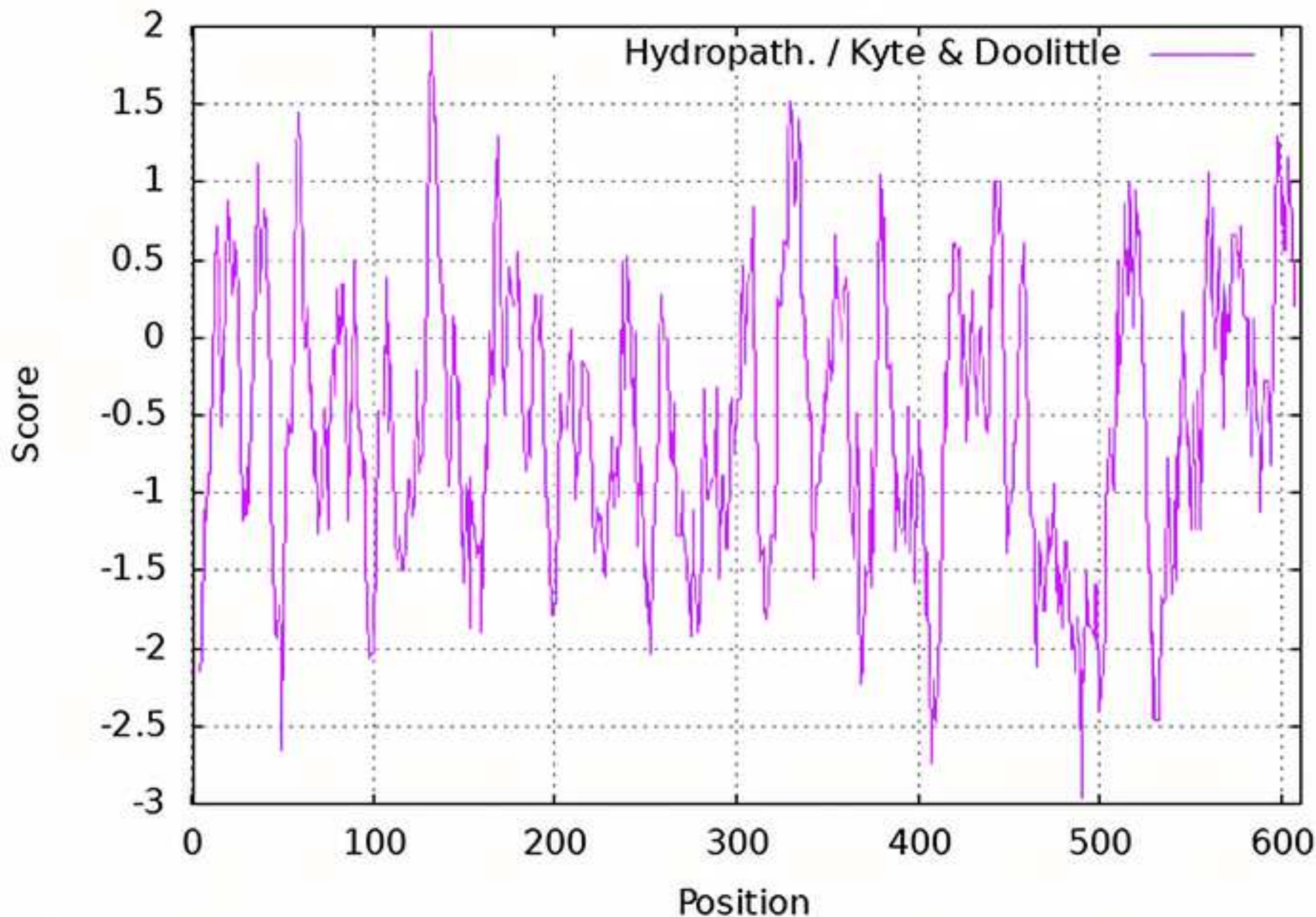
[Click here to access/download;Figure;Figure 3.tif](#)

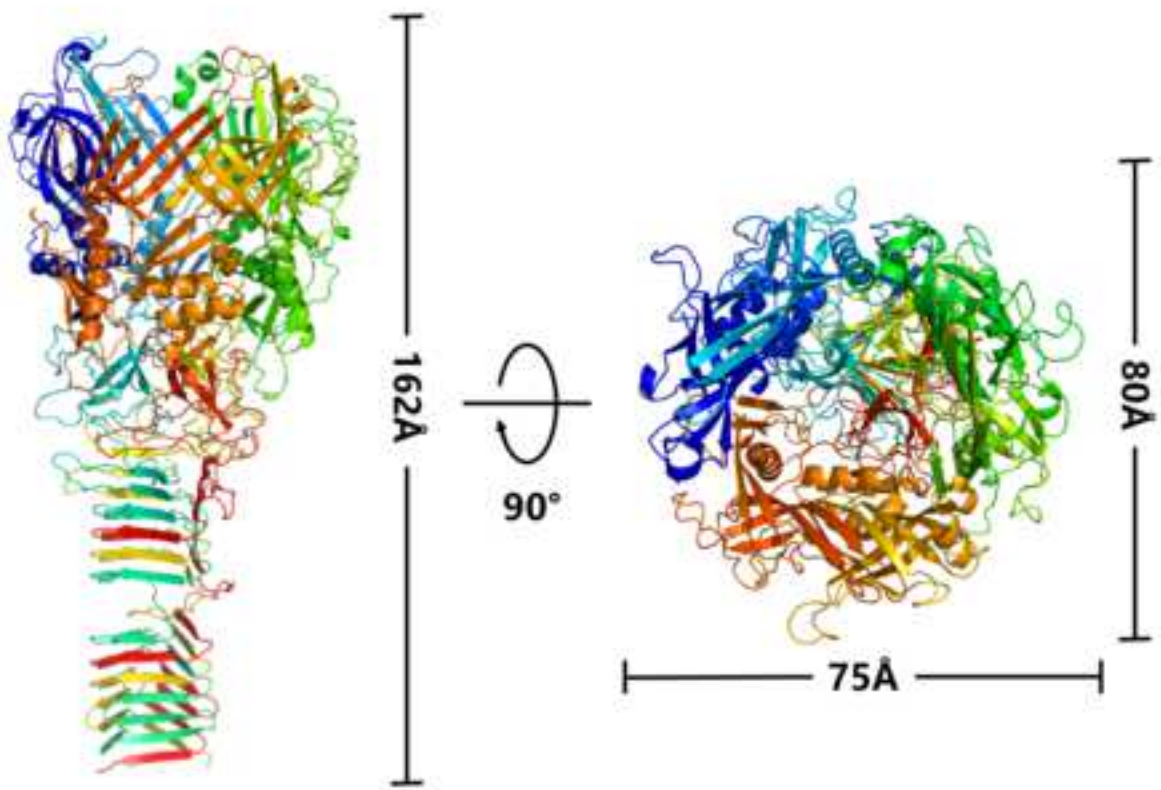
Figure 4

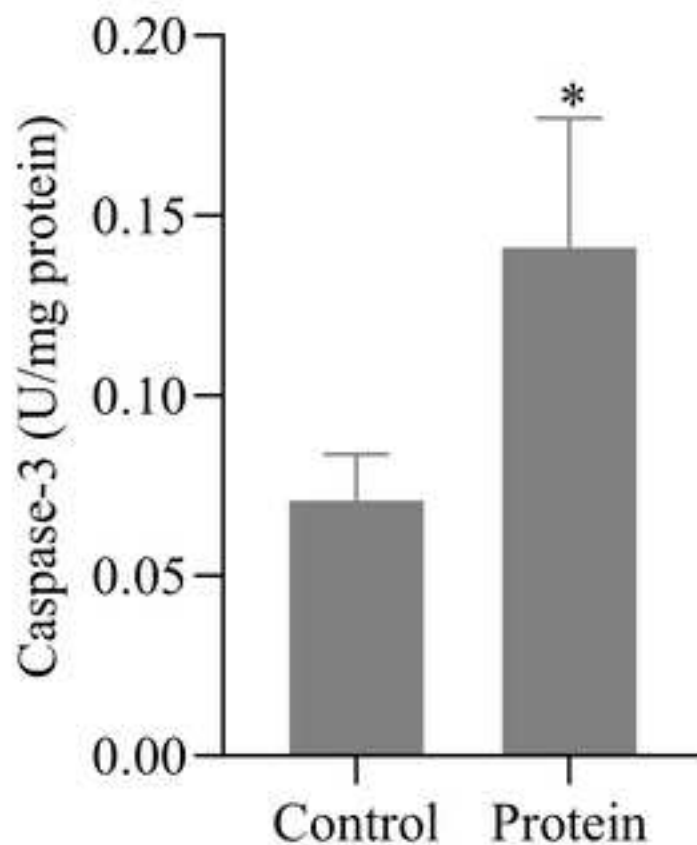
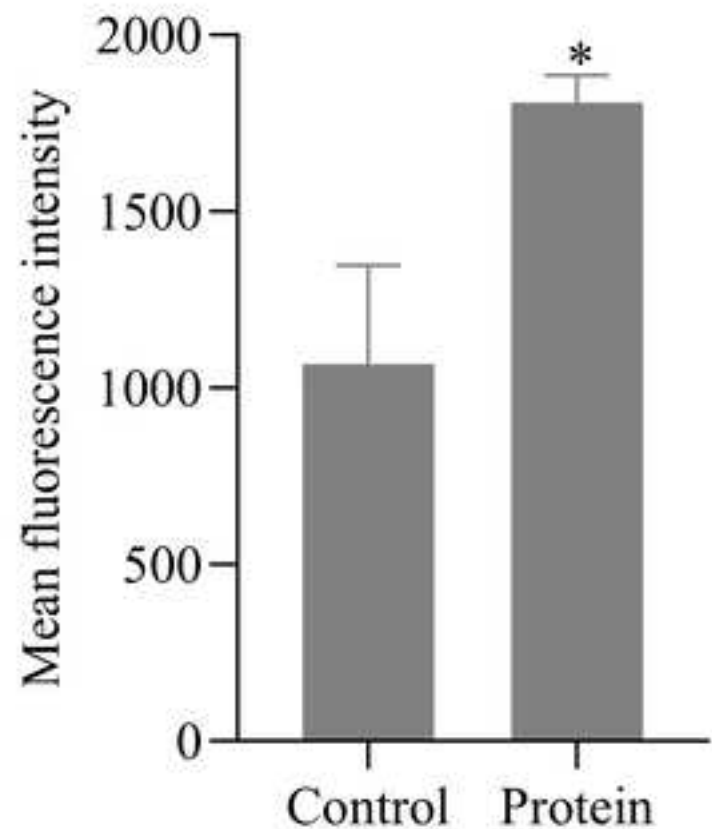
[Click here to access/download;Figure;Figure 4.tif](#)



## ProtScale output for user\_sequence







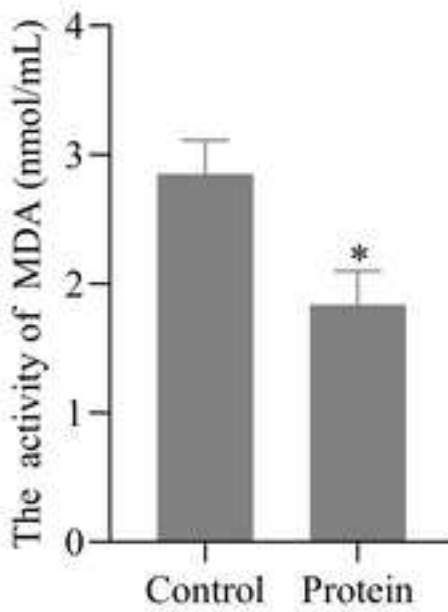
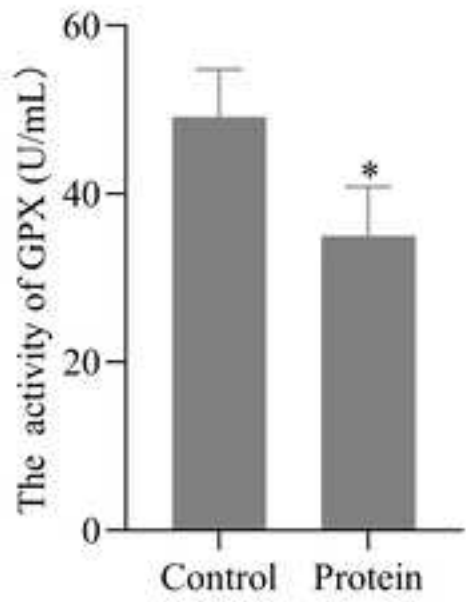
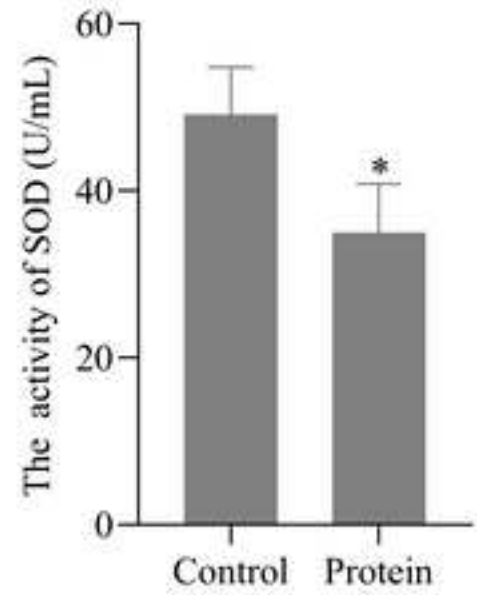


Figure 9

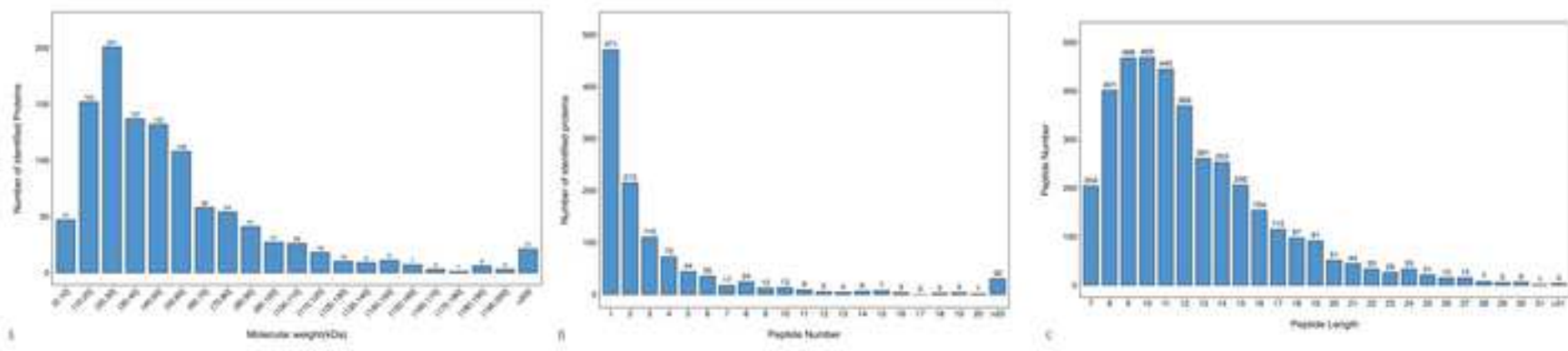
[Click here to access/download;Figure;Figure 9.tif](#)

Figure 10

Click here to access/download;Figure;Figure 10.tif

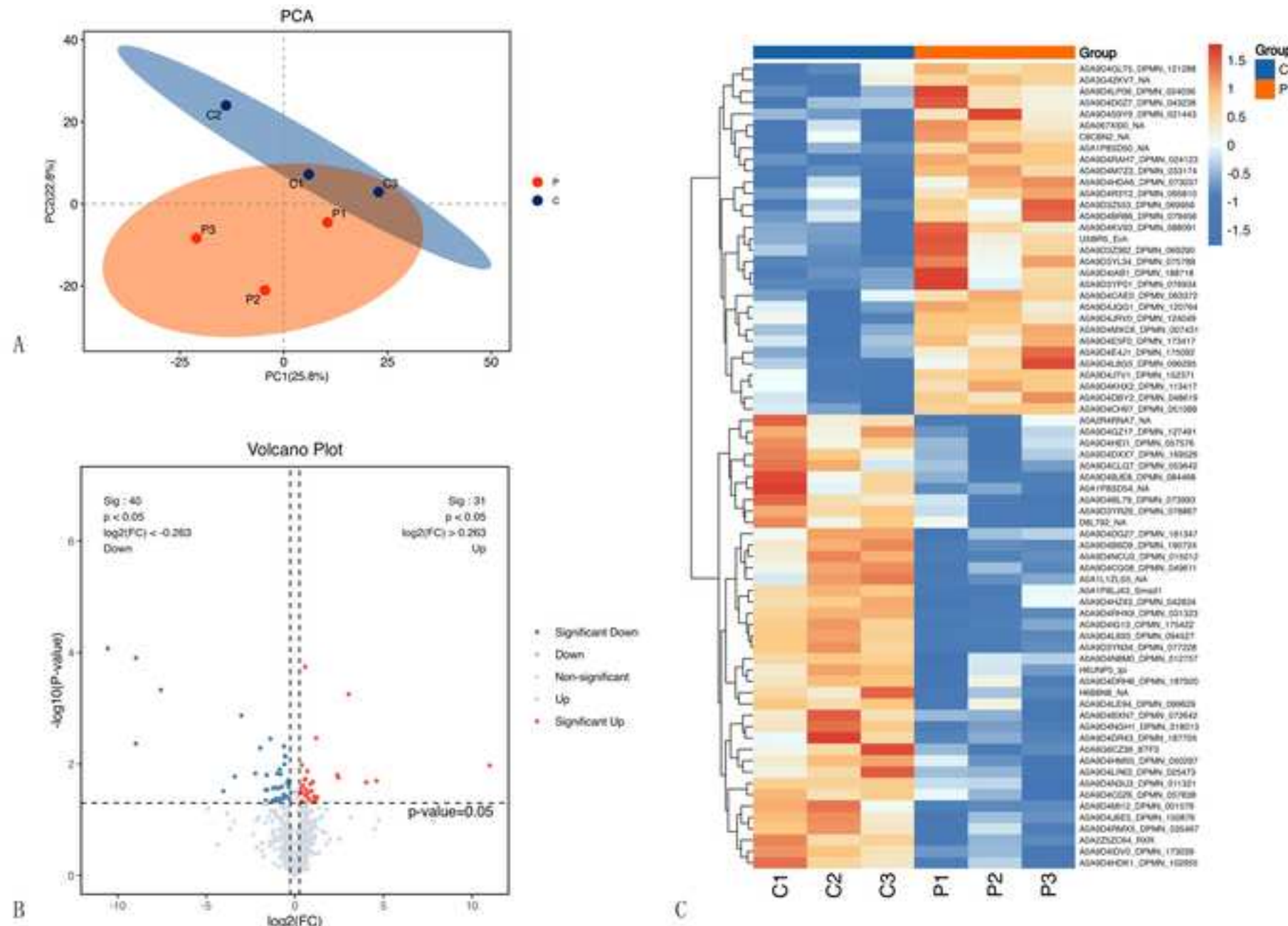
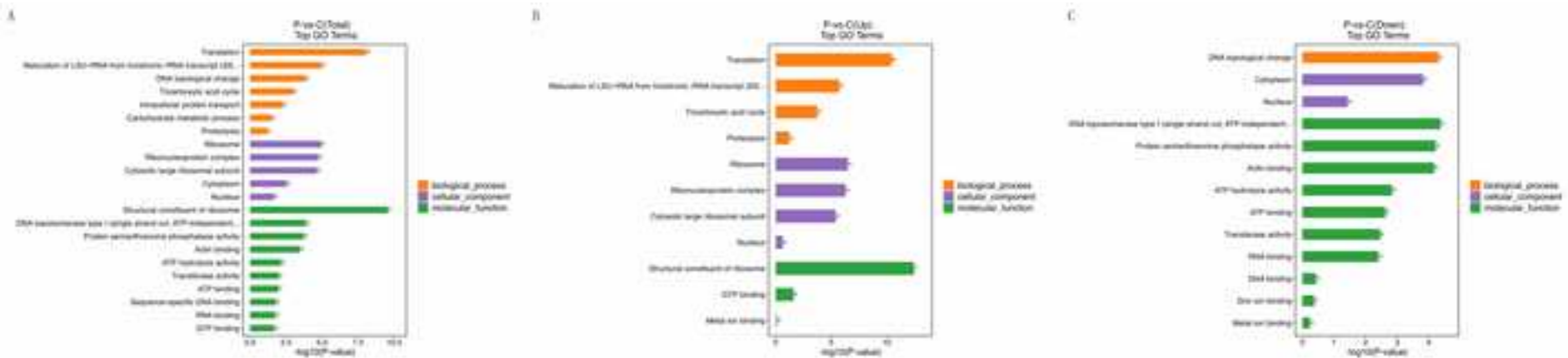


Figure 11

[Click here to access/download;Figure;Figure 11.tif](#)


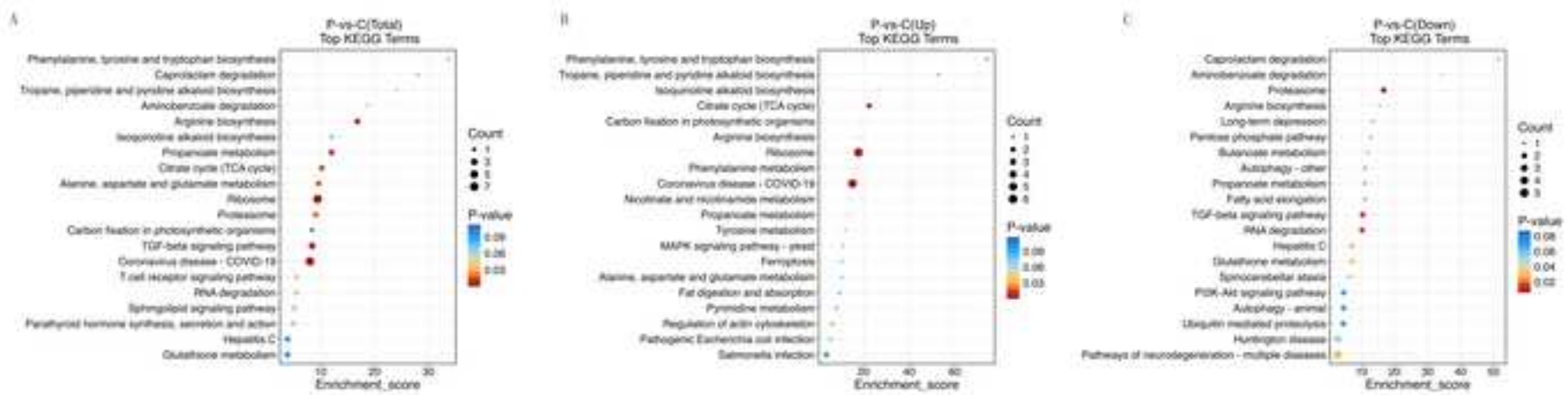


Figure 13

[Click here to access/download;Figure;Figure 13 .tif](#)

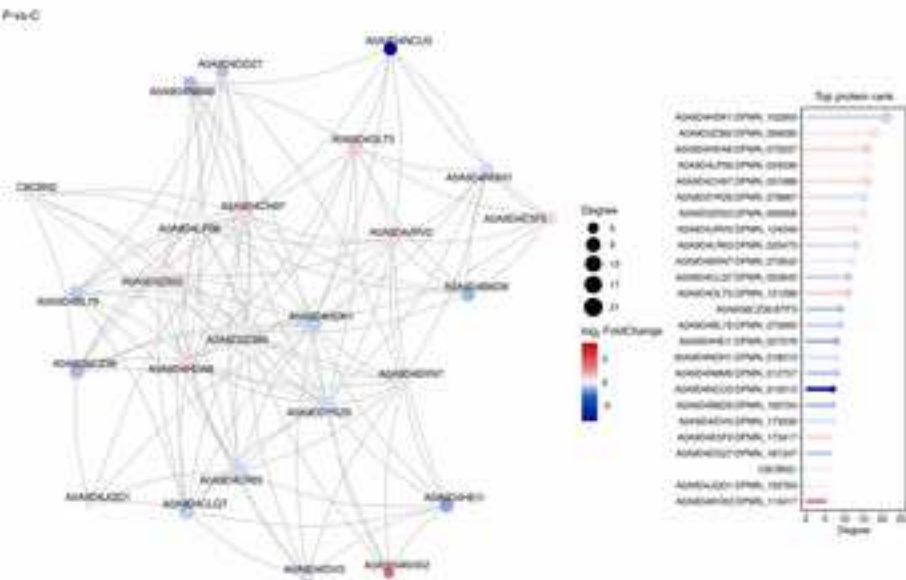
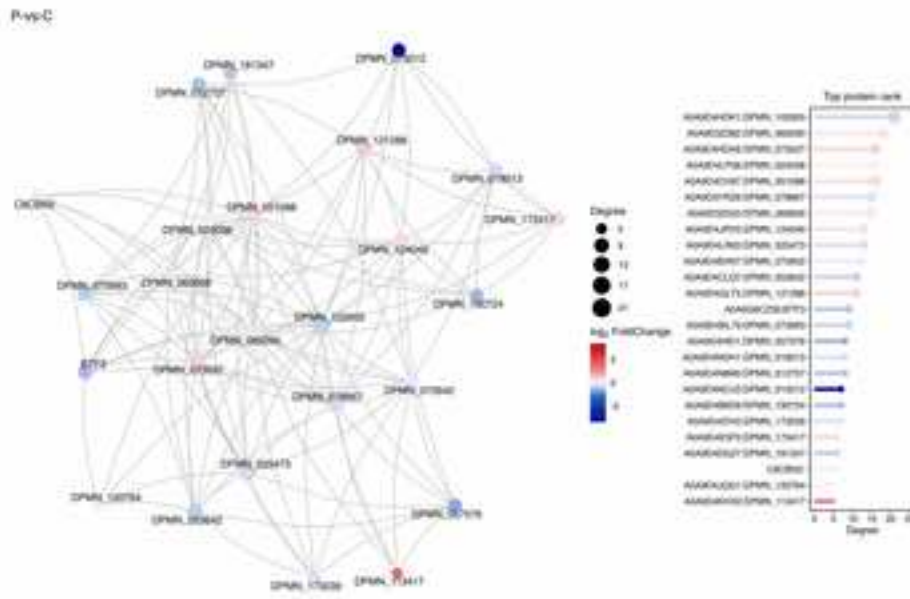
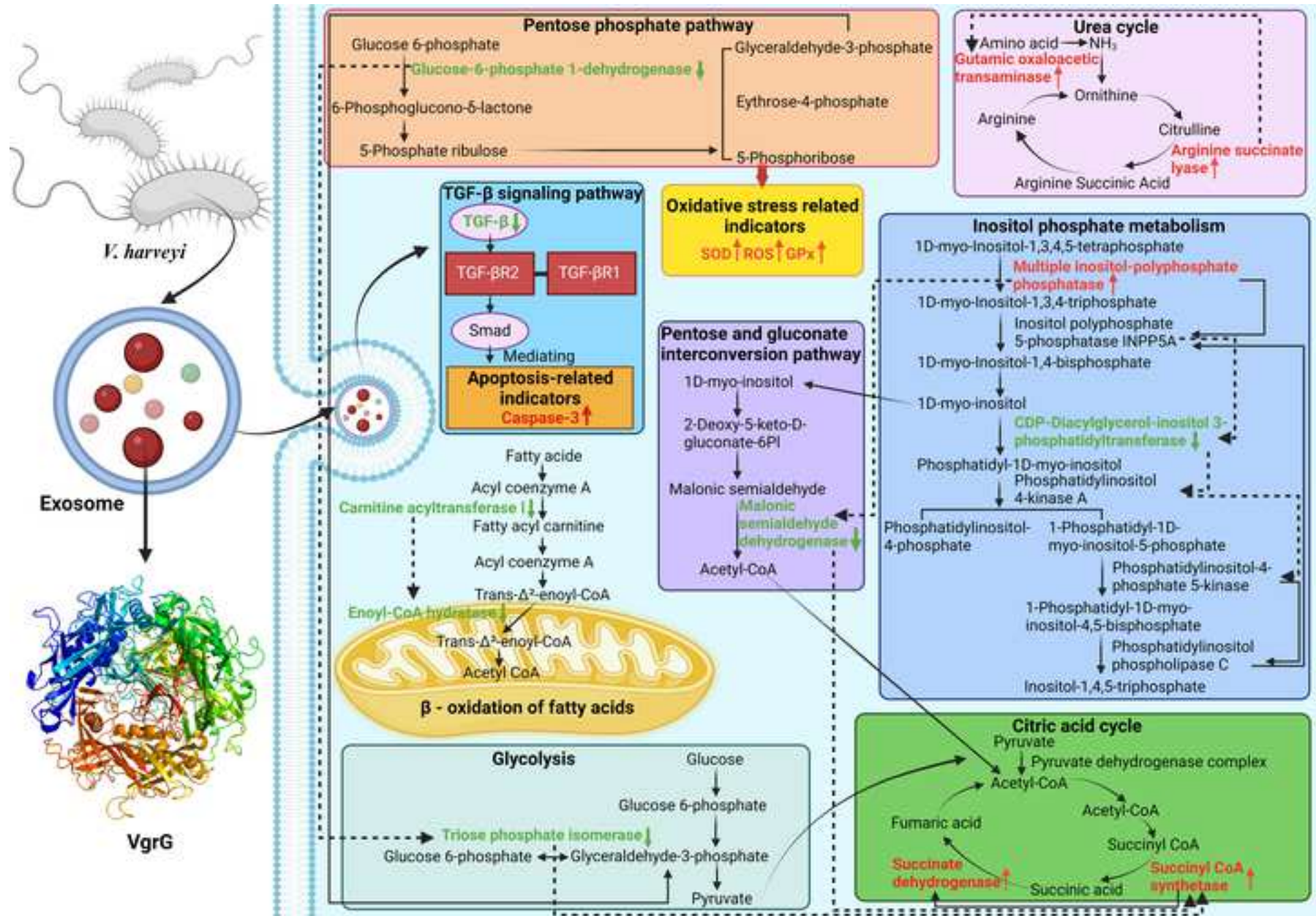


Figure 14

Click here to access/download;Figure;Figure 14.tif



**Declaration of interests**

The authors declare that they have no known competing financial interests or personal relationships that could have appeared to influence the work reported in this paper.

The authors declare the following financial interests/personal relationships which may be considered as potential competing interests:

No If there are other authors, they declare that they have no known competing financial interests or personal relationships that could have appeared to influence the work reported in this paper.